Leader β cells coordinate calcium dynamics across pancreatic islets in vivo

NATMETAB-A18060205A

Supplementary Information

Supplementary Table 1. Ca^{2+} dynamics and connectivity in zebrafish: fast imaging acquisition (frame rate 1 to 3 Hz). T_{20} values, defined as the time taken (s) between glucose injection and the Ca^{2+} intensity spike to reach 20% above baseline for each ROI (cell), are shown. Values corresponding to temporally-defined "leader" cell(s) for a given animal are highlighted in red. See also Figure 5.

Cell/Animal	**# 1**	**# 2**	**# 3**	**# 4**	**# 5**
1	28	34.2	48.3	20.7	18.6
2	23.7	32.7	45.6	24.3	19.5
3	25.5	37.5	48	26.1	19.5
4	25.5	41.1	43.5	33.6	19.2
5	30.6	38.1	48.6	32.1	19.8
6	24	37.2	48.3	31.5	21
7	21.9	27	49.5	21.3	19.5
8	24.6	38.4	51	21.3	19.8
9	23.1		47.7	21.3	21.6
10	26.4		47.7	20.4	20.1
11				24.9	

Supplementary Table 2: Granger connection results for the top four temporally defined “leader cells” in the indicated mouse islets (GCaMP6f driven by the insulin promoter).

Mouse islet (GCaMP6 driven by insulin promoter) [Number of ROIs i.e. cells analysed]	Temporally defined leader cell (numbered 1 – 4 i.e. the first responders to high glucose)	Number of cells to which the temporally-defined leader is causally connected on independent Granger analysis
#1	1	26
	2	26
	3	26
	4	26
#2 [26]	1	26
	2	26
	3	26
	4	26
#3 [44]	1	43
	2	44
	3	44
	4	44
#4 [27]	1	14
	2	13
	3	14
	4	15
#5 [38]	1	33
	2	35
	3	36
	4	36

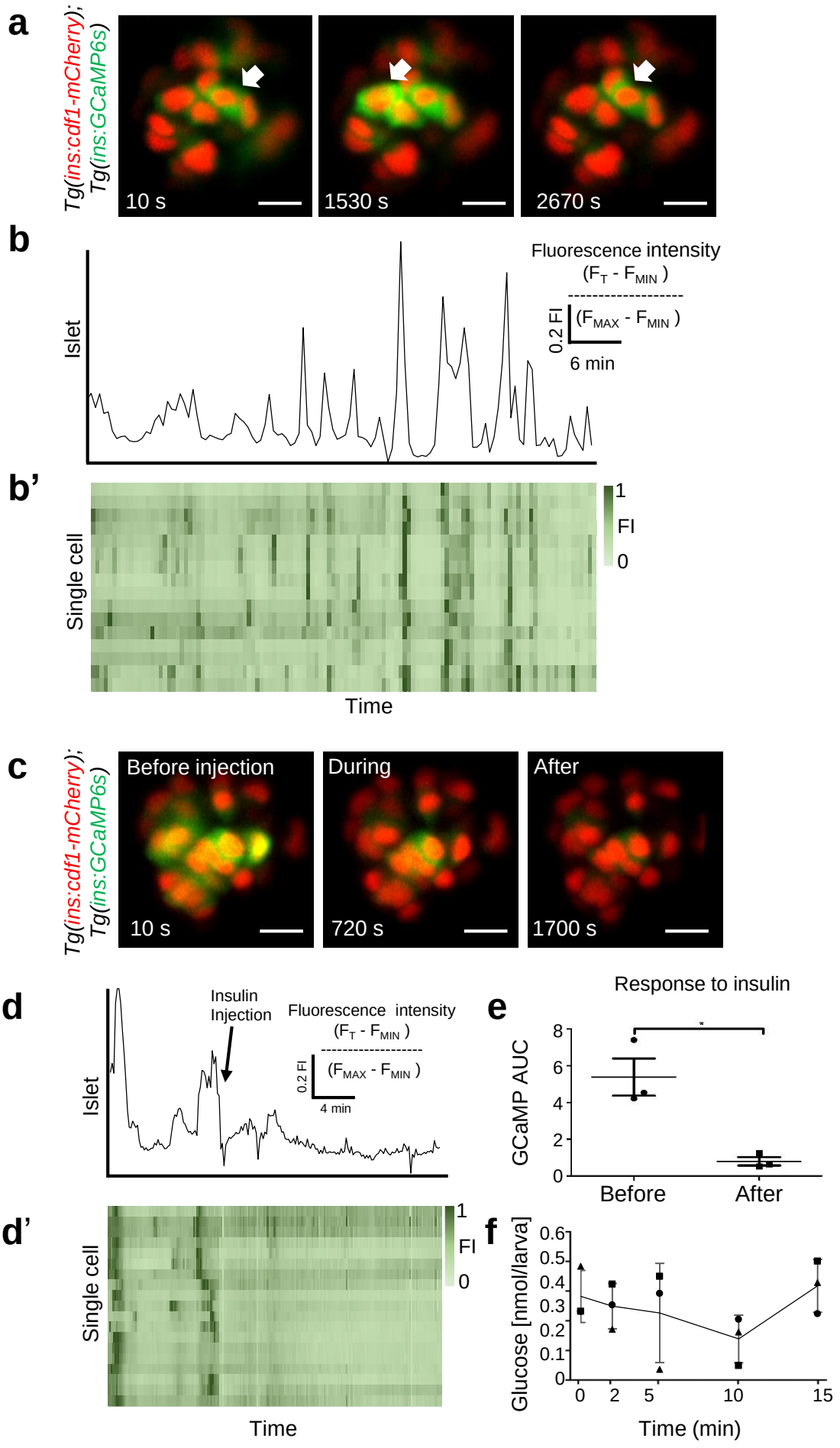

Supplementary Figure 1

Supplementary Figure 1. **Endogenous Ca^{2+} transients imaged in vivo in the living zebrafish: spontaneous Ca^{2+} transients are suppressed by insulin.**

a. Snapshots from time-lapse recordings of the primary islet from a larva mounted in agarose and imaged using a confocal microscope every 30 s. Arrows indicate cells exhibiting an increase in GCaMP6 signal at a given time. The images represent maximum intensity projections. **b.** The top panel shows the trace of cumulative normalized fluorescent intensity over time for the cells shown in b. **b'.** Normalized fluorescence intensity over time for each cell. Each cell is represented by a square. The normalized GCaMP6 fluorescence is displayed as a heat-map, showing the degree of cell activity in individual cells. **c.** Maximum intensity projections of an islet imaged before, during and after the intra-cardiac injection of 5nL of 100 Insulin units/ml of insulin. The imaging and insulin administration were performed simultaneously with a frame rate acquisition every 15 s. **d.** A trace of cumulative normalized fluorescent intensity over time for the cells shown in A. The black arrow marks the instance of insulin injection. **d'.** Normalized fluorescence intensity over time for each individual cell. (*n*=10, not graphically represented here) **e.** Quantification of the islet activity before and after the insulin injection. The graph depicts the GCaMP6 area under the curve covering 100 seconds before and 100 seconds after the insulin injection. The injection of insulin led to a reduction in GCAMP fluorescence intensity (*n*=3 animals, paired two-tailed t-test, P= 0,0476). Data are means ± SD. **f.** Changes in measured free glucose concentration in larvae following insulin injection as in **c**. Each dot represents a pool of 10 injected larvae. . (*n*=3 for each time point, one-tailed ANOVA (with Tukey's multiple comparisons test), P=0,3587). Data are means ± SD Scale bars, 10 μm. The experiments in **a,b** were performed three independent times with several samples showing similar results. The experiments in **c,d** were performed three independent times with several samples showing similar results. **e** shows a quantification from thee biological replicates from one of the repeats. The experiment in **f** was performed one time with several samples.

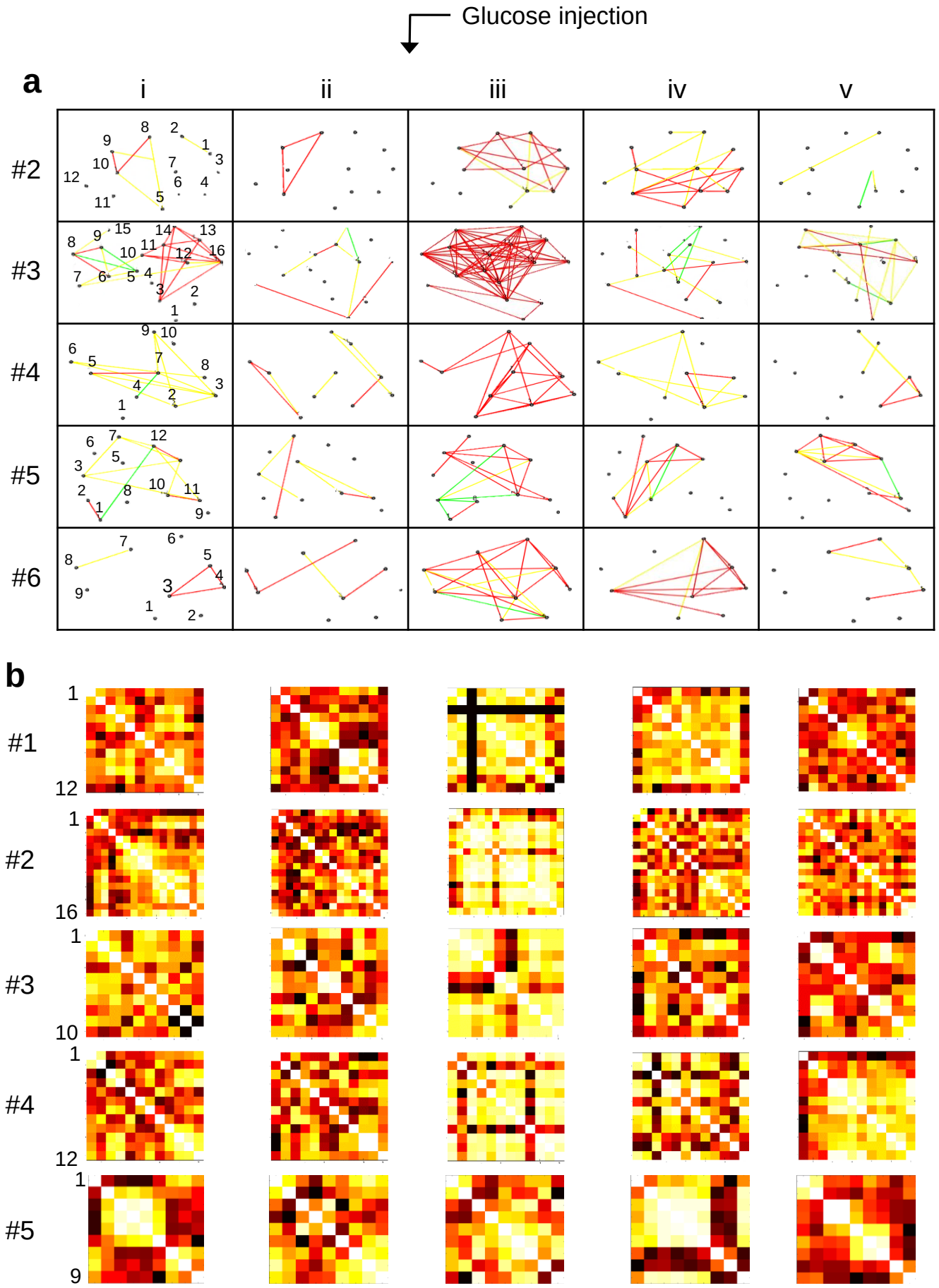

Supplementary Figure 2

Supplementary Figure 2. **Ca^{2+} dynamics and connectivity in zebrafish: slow imaging acquisition (frame rate 0.1Hz).**

a. Cartesian functional connectivity maps displaying the x-y position of analysed cells (numbered black dots). Cells are connected with a coloured line if the p statistic for the Pearson coefficient was < 0.001 post bootstrapping. The strength of the cell pair correlation (the Pearson R statistic) was colour coded: red for R of 0.75 to 1.0, yellow for R of 0.5 to 0.75 and green for R of 0.25-0.5. Results are shown for each of the five time windows that were analyzed (i-v, each 100 secs long) during the 1,200 second imaging period. The middle time window, iii, occurred during glucose injection. Results confirm an increase in cell-cell connectivity (strength AND number) during glucose injection (grouped in Main Figure 2 E and F). **b.** Heat maps show the Pearson coefficient of each cell pair in a colour-coded manner (negative correlation; dark brown (-1), no correlation; mid brown (0), high correlation; yellow/white (1)), across the five time windows (two before and two after glucose injection). (*n*=6).

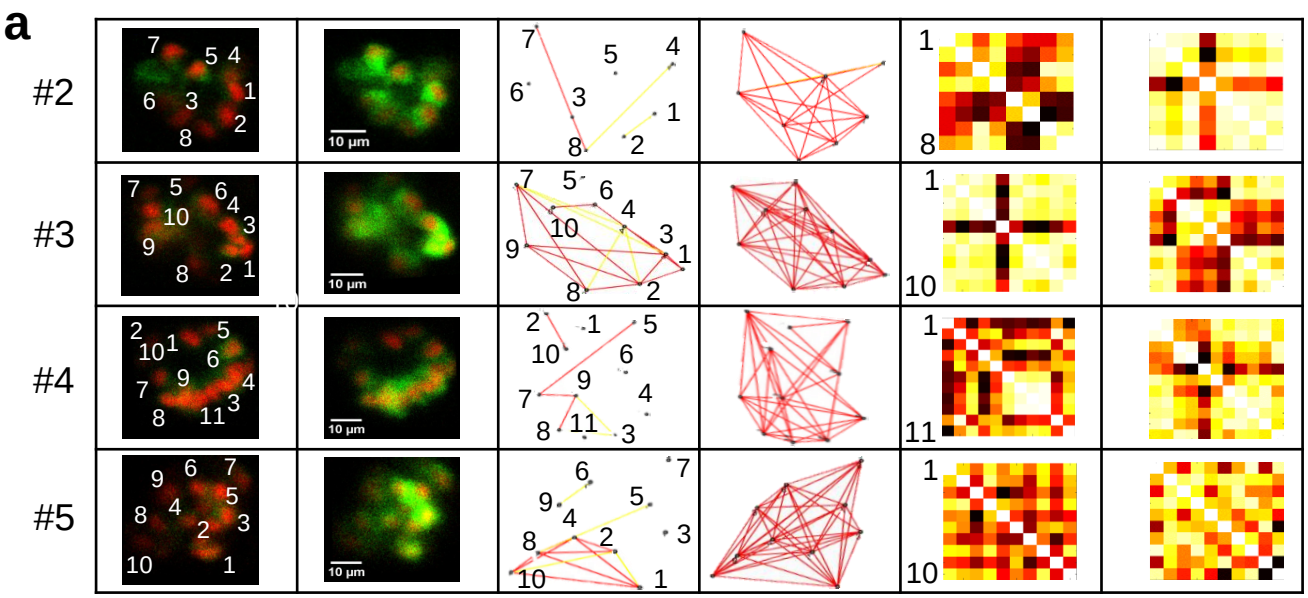

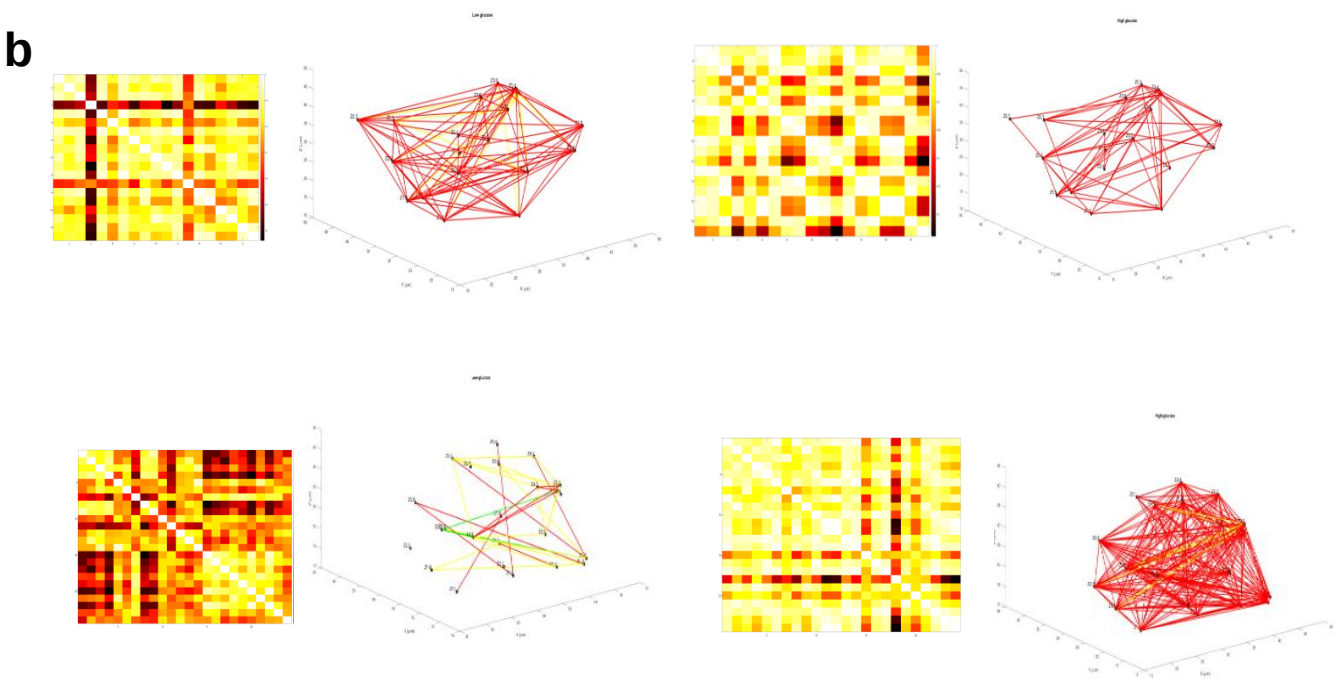

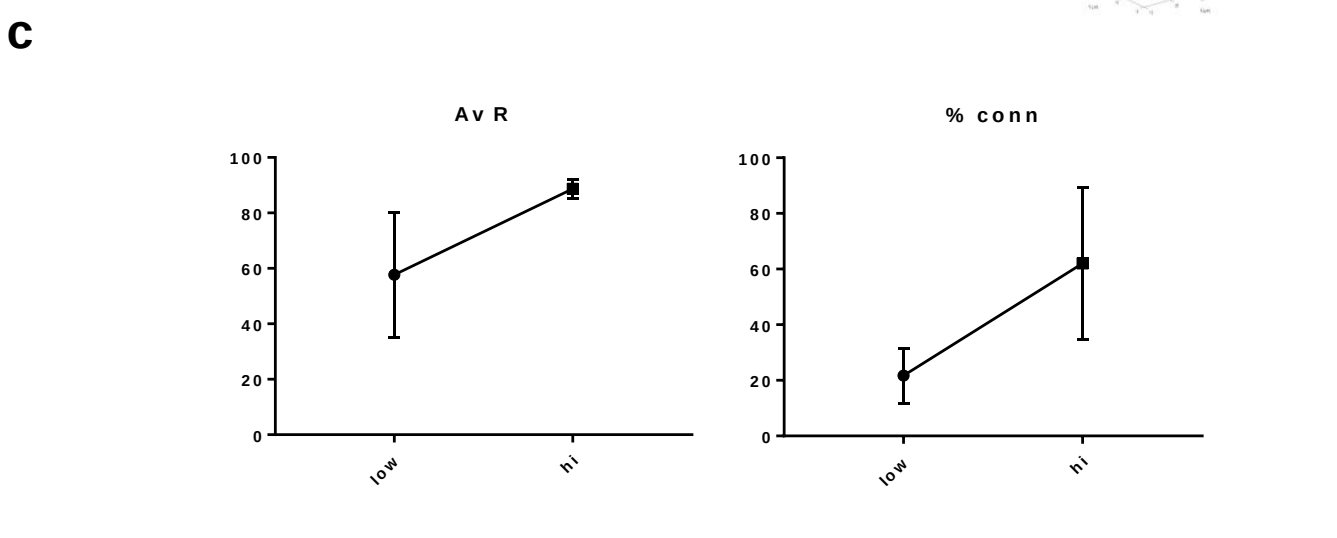

Supplementary Figure 3

Supplementary Figure 3. **Islet connectivity in 2D and 3D.**

a. Cartesian connectivity maps and Pearson heatmaps for the remaining animals corresponding to the 2D imaging and analysis shown in Figure 3 a-d (*n*=5 for total experiment).

b. Cartesian connectivity maps and Pearson heatmaps for the remaining animals corresponding to the 3D imaging and analysis shown in Figure 3 e-f (*n*=6 for total experiment).

c. The percentage of connected cell pairs imaged in 3D increases following glucose administration (*n*=3). Data are means ± SEM.

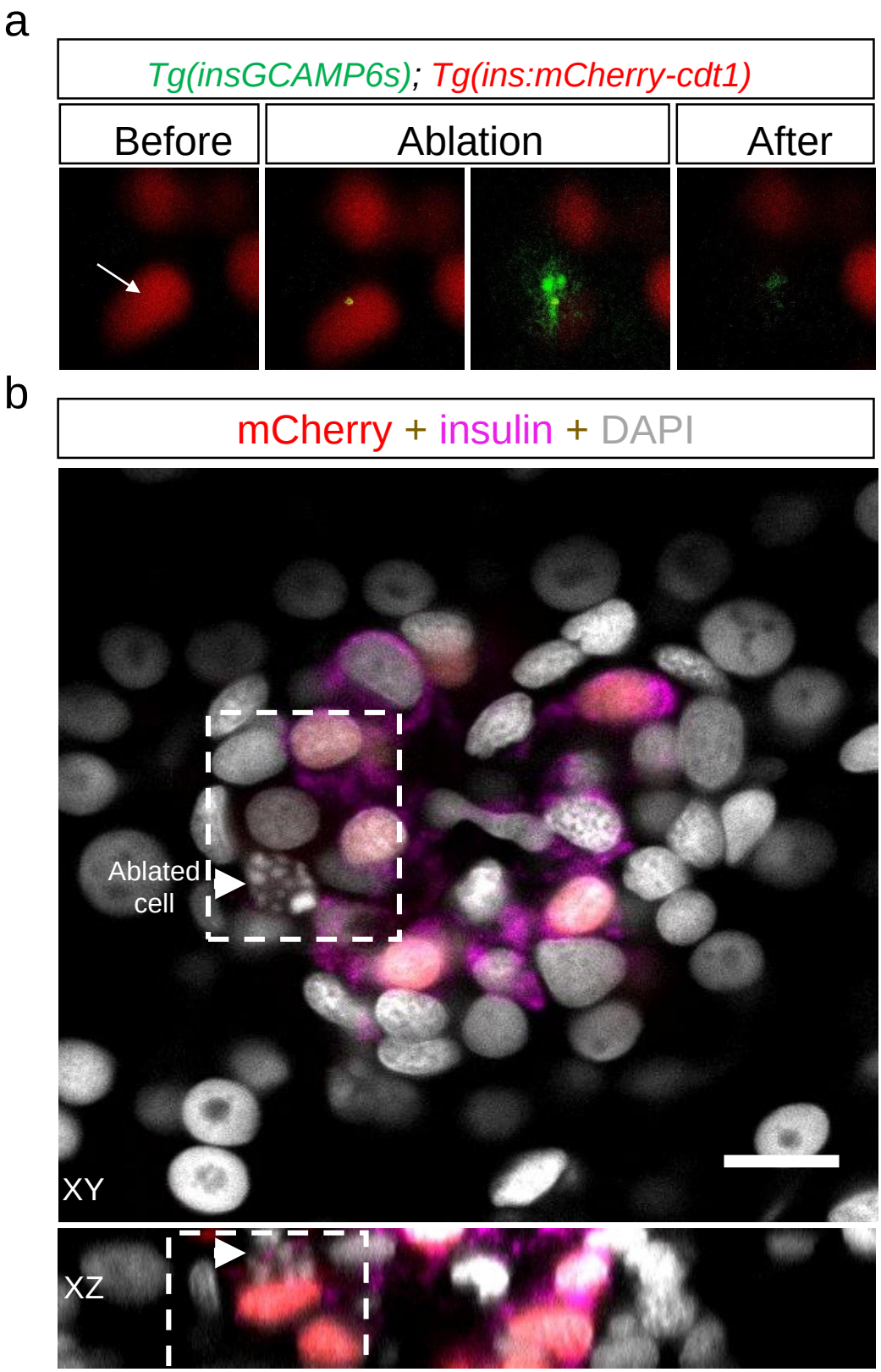

Supplementary Figure 4

Supplementary Figure 4. **2-Photon UV ablation achieves highly targeted, single cell destruction.**

a. Images of a time-lapse recording in a single plane of a cell undergoing laser ablation (arrow). The snapshots show the nuclei of β-cells marked using *Tg(ins:mCherry-cdt1)* before, during and after the ablation of the targeted cell. **b**. Confocal image corresponding to the islet showed in a, following fixation and immunohistochemistry against Insulin. Arrow marks the damaged nucleus of the ablated cell. The DAPI staining showed no discernible damage to neighbours cells (*n*=5). Scale bar = 10µm. The experiment was performed on one occasion with five samples showing similar results.

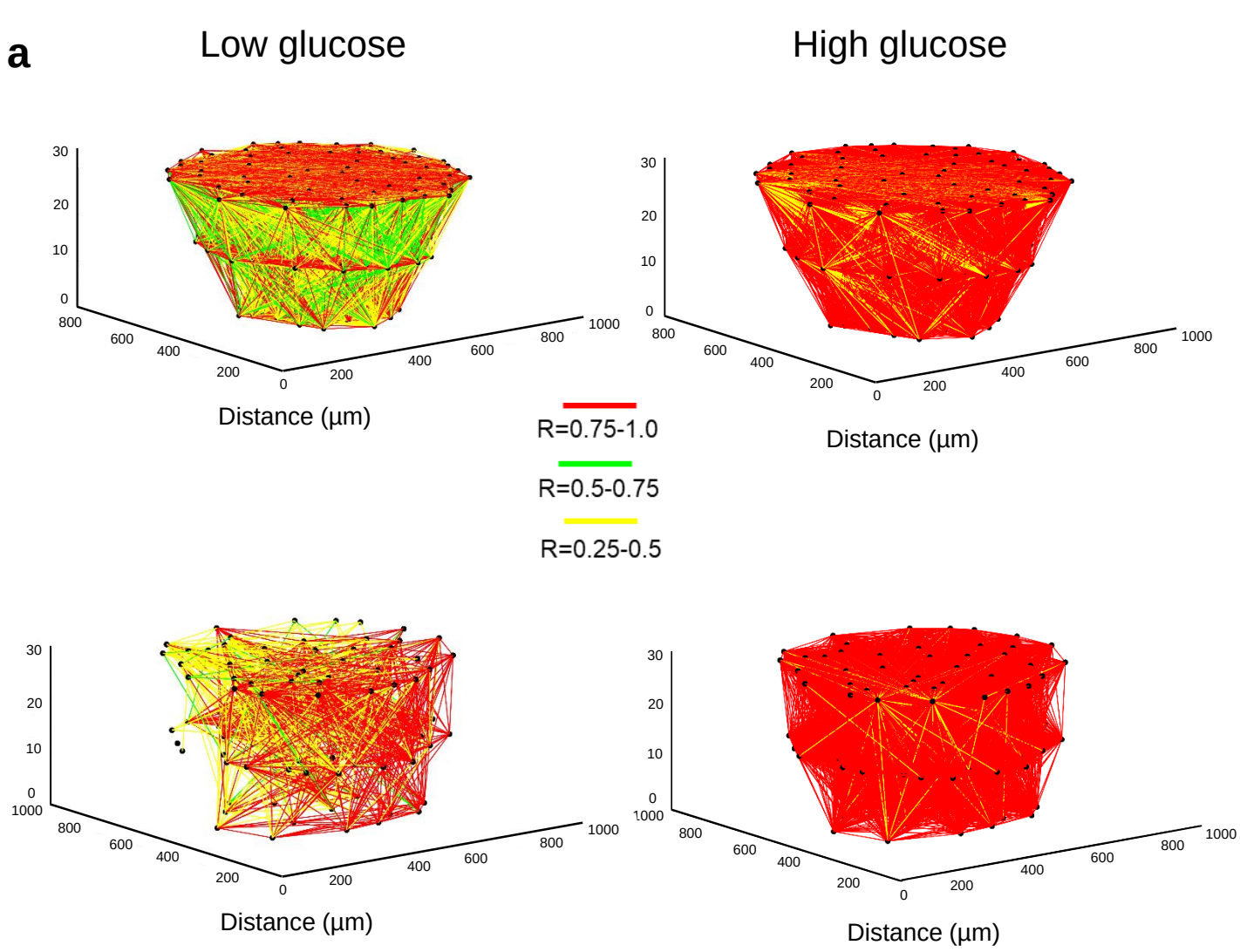

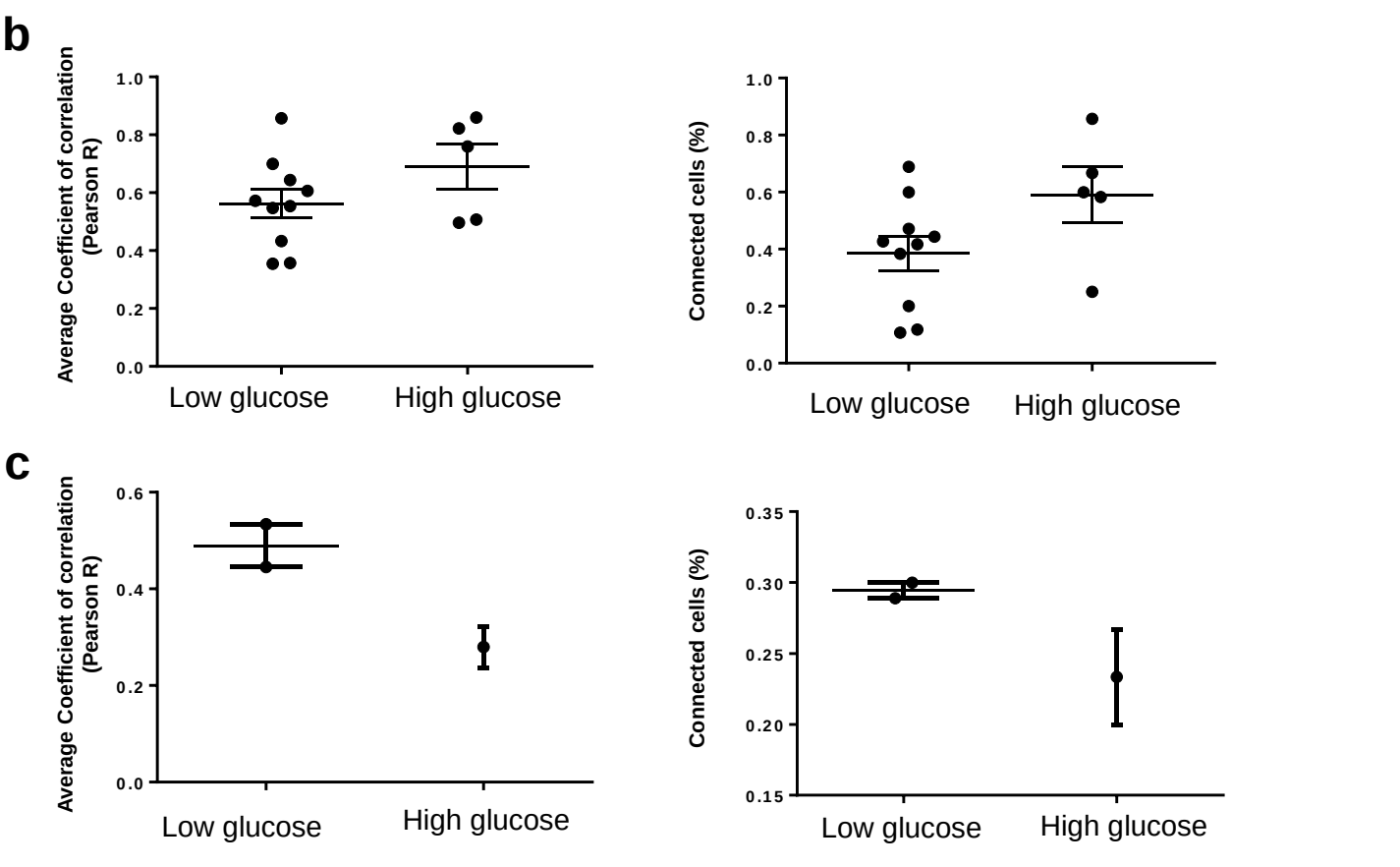

Supplemental Figure 5

Supplementary Figure 5: **Ca^{2+} dynamics and connectivity in mouse islets expressing GCaMP6f under the Insulin promoter. a.** 3D Cartesian connectivity maps and (as previously described in Supplementary Figure 2) for the remaining 2 animals not shown in Figure 5, in low *versus* high glucose states. A total of 3 islets in 3 different animals were used for this group of experiments. **b.** Pooled data for average R and % connectivity measurements in healthy human islets transplanted infected with AV-GCaMP6 and transplanted into Balb/c nu/nu recipient mice. A non-significant (on two-tailed unpaired t test) trend in increase in both indices is observed between low and high glucose levels. Healthy human islets (11 experiments) came from four individual human donors: 1. male, age at death 74, BMI 29.2; 2. male, age at death 14, BMI 21.5; 3. female, age at death 65, BMI 28.8; 4. male, age at death 50, BMI 22.9, died of cardiovascular disease. Individual data points are shown for each experiment. There are fewer data points for the “high” glucose condition because the mice did not always respond with a robust rise in glucose under the anaesthetic conditions. **c.** Two islets from a single human diabetic donor were transplanted individually. Both exhibited a reversal in trend for connectivity, which dropped from the low to high glucose state. Donor details: female, 54 years old, BMI 24.4, type 2 diabetic for 10 years, insulin dependent for the last 1.5 yrs.

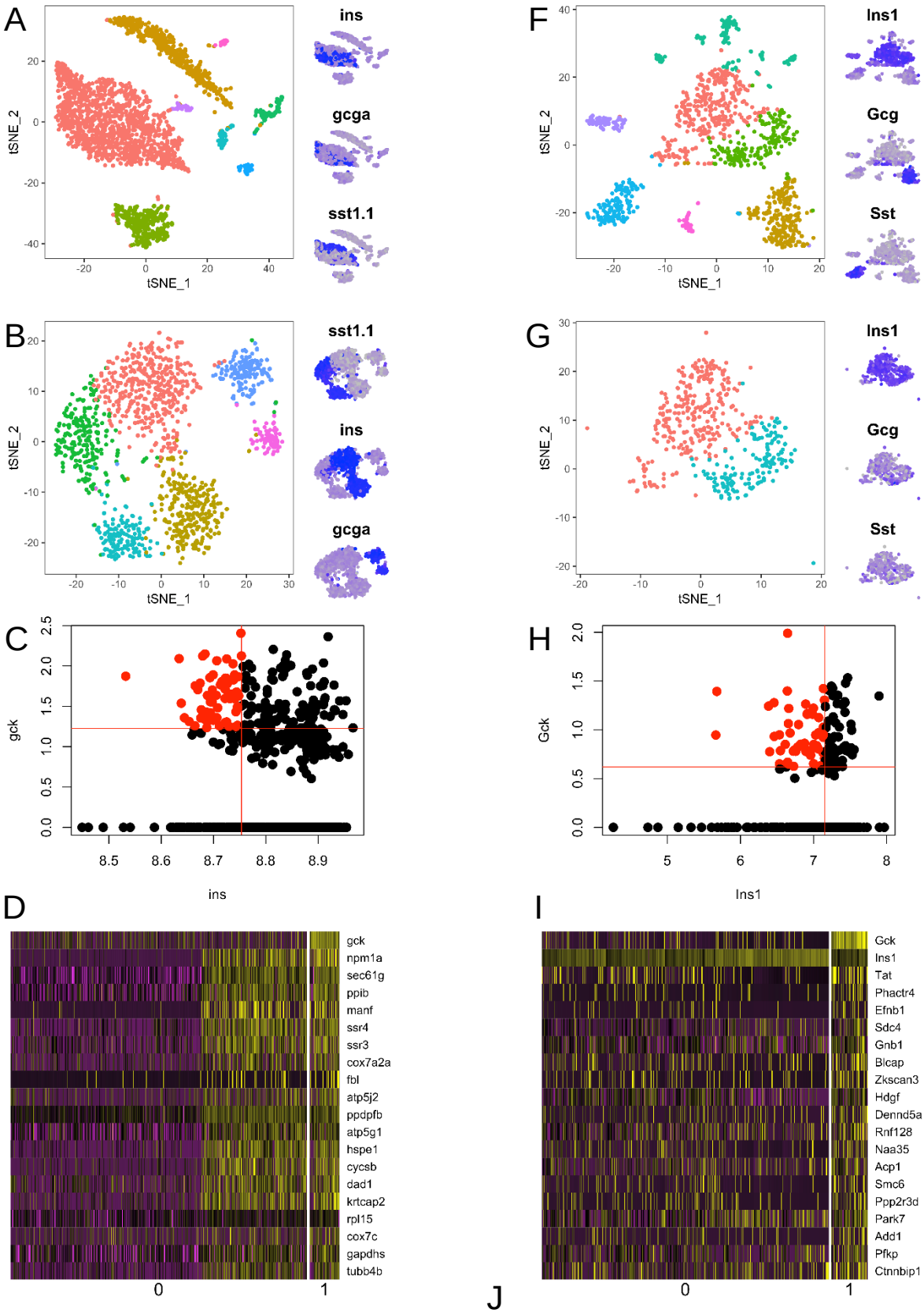

E

GO BP	Fold Enrichment	FDR
oxidative phosphorylation	21.53	1.84E-09
respiratory electron transport chain	12.49	7.55E-09
generation of precursor metabolites and energy	9.10	5.53E-09
protein folding	8.04	5.73E-05
RNA localization	7.27	6.78E-03

J

GO BP	Fold Enrichment	FDR
glycolysis	17.28	1.54E-02
generation of precursor metabolites and energy	6.04	1.81E-02

Supplementary Figure 6

Supplementary Figure 6. **Single Cell RNA-Seq analysis of Zebrafish (a-e) and Mouse (f-j) islets to identify putative hub/leader cells. a.** t-distributed Stochastic Neighbor Embedding (TSNE) plot of initial clustering of Zebrafish islet cells shows insulin, glucagon and somatostatin-positive cells all contained in a single 'endocrine' cluster. **b.** Subsequent re-clustering of this 'endocrine' cluster separates into distinct clusters expressing insulin, glucagon and somatostatin. **c.** The pooled insulin-positive clusters were filtered to remove the few cells expressing other hormones then putative hub cells (red) were identified on the basis of higher *gck* expression and lower *ins* expression (see Results) (*n*=6 animals yielding 2625 cells). **d.** Heatmap showing the top 20 genes defining the putative hub cells. **e.** Statistically over-represented GO BP terms in genes upregulated in putative hub cells. **f.** Initial clustering of mouse islet data shows distinct clustering of cells expressing insulin, glucagon and somatostatin. **g.** The majority of insulin- positive cells were contained within the two central clusters showing little expression of the other two hormones. **h-j** The identified mouse β cells were analysed in a similar manner to the Zebrafish cells to identified genes defining putative hubs and overrepresented GO BP terms.